© 2022. Published by The Company of Biologists Ltd | Journal of Experimental Biology (2022) 225, jeb244518. doi:10.1242/jeb.244518

RESEARCH ARTICLE

Thermal sensitivities of respiration and protein synthesis differ among larval families of the Pacific oyster, *Crassostrea gigas*

Melissa B. DellaTorre, Francis T. C. Pan, Andrew W. Griffith, Ning Li and Donal T. Manahan*

ABSTRACT

Understanding the mechanisms of biological responses to environmental change is a central theme in comparative and evolutionary physiology. Here, we analyzed variation in physiological responses to temperature, using 21 full-sibling larval families of the Pacific oyster, *Crassostrea gigas*. Pedigrees were confirmed with genetic markers for adult broodstock obtained from our breeding program. From these 21 larval families, 41 determinations of thermal sensitivity (Q_{10} values) were assayed for larvae of different sizes. For respiration, thermal sensitivity was consistent within a larval family during growth, but showed significant differences among families. Different Q_{10} values were evident among 21 larval families, with family accounting for 87% of variation. Specifically, four larval families maintained an increased thermal sensitivity for respiration (Q_{10} of 3). This physiology would confer resilience to rising temperature by matching the increased energy demand of protein synthesis (Q_{10} of 3 previously reported). For protein synthesis, differences in Q_{10} values were also observed. Notably, a family was identified that had a decreased thermal sensitivity for protein synthesis (Q_{10} of 1.7 cf. Q_{10} of 3 for other families), conferring an optimal energy allocation with rising temperature. Different thermal sensitivities across families for respiration (energy supply) and protein synthesis (energy demand) were integrated into models of energy allocation at the whole-organism level. The outcome of these analyses provides insights into the physiological bases of optimal energy allocation with rising temperature. These transgenerational (egg-to-egg) experiments highlight approaches to dissect components of phenotypic variance to address long-standing questions of genetic adaptation and physiological resilience to environmental change.

KEY WORDS: Biosynthesis, Development, Metabolism, Oyster, Temperature

INTRODUCTION

Animals differ in their range of temperature tolerances throughout their life-history, and across latitudes and ocean depths (Schmidt-Nielsen, 1997; Pörtner, 2002; Somero et al., 2017). Early developmental stages, including larval forms, are often more vulnerable to temperature and other environmental perturbations than are adult stages (Pörtner and Knust, 2007; Dupont et al., 2010; Ross et al., 2011; Dahlke et al., 2020). Mechanisms for varied thermal tolerance across life stages and life spans are often related to bioenergetics of stress tolerance (Hand and Hardewig, 1996; Sokolova et al., 2012; Sokolova, 2021). While many studies focus on increases in metabolic rate in response to temperature increase, a major question remains as to which physiological systems are responsible for setting thermal limits (Somero, 2010). Models of oxygen supply and demand for marine animals currently predict an imminent mass extinction due to the acceleration of ocean warming (Penn and Deutsch, 2022). Understanding the mechanisms of physiological plasticity is a basis for better predictions of resilience to environmental change (Melzner et al., 2009; Seebacher et al., 2015; Tresguerres, 2016). Phenotypic variation resulting from genetic variation will ultimately dictate long-term evolutionary responses (a focus of the present study).

Regulation of respiration rate (energy supply) and protein synthesis rate (energy demand) are two critical processes for maintaining energy balance in an organism. Protein synthesis is one of the most energetically costly processes in cellular biology (Siems et al., 1992; Wieser and Krumschnabel, 2001; Cherkasov et al., 2006). For developmental stages of marine invertebrates, over 50% of the total pool of adenosine triphosphate (ATP) can be allocated to the single process of protein synthesis (e.g. white sea urchin *Lytechinus pictus*: Pace and Manahan, 2006; purple sea urchin *Strongylocentrotus purpuratus*: Pan et al., 2015; Pacific oyster *Crassostrea gigas*: Frieder et al., 2018). The thermodynamic cost of synthesizing a unit-mass of protein for larvae of *C. gigas* has previously been determined and, notably, this cost is fixed and independent of environment, genotype and phenotype (Lee et al., 2016).

Proteins are constantly degraded and recycled in organisms, and the functioning of protein synthesis is essential for maintaining homeostasis for growth and development under changing environmental conditions (Hawkins, 1991; Tsukada and Ohsumi, 1993; Vavra and Manahan, 1999; Frieder et al., 2018). Environmental stress results in changes in the allocation of energy in marine invertebrate larvae. In larvae of the sea urchin *S. purpuratus*, for instance, significant increases were measured in ATP allocation to support the cost of increased protein synthesis and turnover under conditions of ocean acidification (Pan et al., 2015). Larvae of the oyster *C. gigas* also had increased rates of protein synthesis and turnover under conditions of ocean acidification (Frieder et al., 2018). In that study, Frieder et al. (2018) reported different strategies used by larvae to support the increased demand for protein synthesis – reallocating a larger portion of the available ATP pool, or increasing metabolic rate to increase available ATP. Changes in the bioenergetic allocation of ATP were further analyzed for *C. gigas* larvae, where thermal sensitivity (measured as Q_{10} value) for respiration was reported to have a lower Q_{10} of ∼2 than the Q_{10} for protein synthesis of ∼3 (Pan et al., 2021). The differential thermal sensitivities of supply and demand of the ATP pool have implications for larvae experiencing different scenarios of

Department of Biological Sciences, University of Southern California, Los Angeles, CA 90089-0371, USA.

*Author for correspondence (manahan@usc.edu)

M.B.D., 0000-0001-5114-1901; F.T.C.P., 0000-0002-1550-4581; A.W.G., 0000-0001-9157-4242; N.L., 0000-0002-5080-5726; D.T.M., 0000-0002-6437-9107

Received 6 May 2022; Accepted 24 October 2022

rising temperature, as the energy demand of biosynthesis would increase at a greater rate (higher Q_{10} value) than the ability to supply energy. This imbalance would result in an increased – and eventually unsustainable – allocation of available ATP to protein synthesis. Of note is that the disproportionate increase in the energy demand of protein synthesis is a result of the higher thermal sensitivity of the rate of protein synthesis per se, not a change in the energy cost per unit-mass of protein synthesized (the latter cost is temperature independent: Lee et al., 2016). As with many evolutionary scenarios there may, however, be sufficient standing genetic variation to provide physiological variance within a population of a given species that could confer resilience to environmental change. This is the focus of the present study.

Studies of variation in respiration have mostly focused on environmental influences. Dissecting the complex contributions of 'nature versus nurture' is challenging in animal developmental physiology (Applebaum et al., 2014). For species with well-developed genetic resources, there is genetic variance in respiration and metabolic responses to temperature (Einum et al., 2019; Fossen et al., 2019). Among different lines of the fruit fly *Drosophila melanogaster*, adaptation to temperature change alters the relationship between metabolism and growth rate (Williams et al., 2016), with different lines having complex interactions between the thermal sensitivity of metabolic rate and heat tolerance (Berrigan and Partridge, 1997; Folk et al., 2007). In the present study, a series of crosses were undertaken with (single) male and female, pairwise matings of the Pacific oyster, *Crassostrea gigas*, to study the temperature physiology of 21 distinct larval families. The genealogical record of each parent used in crosses was confirmed by genotyping, based on analyses of single-nucleotide polymorphisms (SNPs). We report that several larval families have the physiological capacity to increase respiration rate with a Q_{10} of 3, to match the same high Q_{10} value for thermal sensitivity of protein synthesis (previously reported by Pan et al., 2021). In addition, we present a novel finding of an alternative mechanism to reduce the high cost of living under thermal stress – a lowering of the thermal sensitivity (Q_{10} less than 2) of protein synthesis. We summarize these findings in bioenergetic models of ATP trade-offs that have implications for resilience to rising temperature.

MATERIALS AND METHODS

Genotyping of adult broodstock

Parental samples for all individuals used in crosses were genotyped by high-resolution melting of SNP-containing amplicons, following the methods in Sun et al. (2015). These mapped genetic markers in the genome are referred to as composite SNP markers (or simply 'markers'), because most amplicons contain multiple SNP sites and are multi-allelic in contrast to single, bi-allelic SNP markers. Individual adults in the present study were genotyped at 45 different markers (Sun et al., 2015). For genotyping in the present study, to confirm parentage, over 1700 PCRs were conducted from tissue samples taken from adult broodstock, each tested at 45 SNP markers for determination of genotype. Gravid adult broodstock of the Pacific oyster, *Crassostrea gigas* (Thunberg 1793), were obtained from our transgenerational ('egg to egg') breeding program to establish different lines from wild populations (see similar approaches in Hedgecock et al., 1995; Pace et al., 2006; Hedgecock and Davis, 2007). To confirm parentage, each animal was briefly treated with a solution of $MgSO_4$ (Epsom salt, added to seawater at 73 g l^{-1}) to relax the adductor muscle and allow a sample of mantle tissue to be taken. Tissue was preserved in 70% ethanol and DNA was extracted using standard protocols (DNeasy Blood & Tissue, Qiagen, Germantown, MD, USA).

High-resolution melting assays were based on amplification of SNP-containing sequences by PCR, followed by one cycle of cooling and heating to determine the melting temperature of sequences containing different SNPs (Sun et al., 2015). Each reaction had a final volume of 10 µl, consisting of 1 µl DNA, 0.35 µl forward and reverse primers, 1.2 µl $MgCl_2$, 2.45 µl molecular grade H_2O and 5 µl of the high-resolution melting Master Mix (Roche Diagnostics, Indianapolis, IN, USA). Target amplicons were amplified by PCR in 384-well plates, using a LightCycler 480 thermocycling instrument (Roche Diagnostics) using reaction conditions given by Sun et al. (2015). Following PCR amplification, products were denatured at 95°C for 1 min, cooled to 40°C, and then heated gradually, at a rate of 0.05°C s^{-1}, to a target temperature of 95°C. Fluorescence (SYBR Green) was monitored in each well during heating. Genotypes were determined by examining the normalized melting curves, using LightCycler 480 software (v1.5) Gene Scanning 384-II module.

Parental genotypes were compared with the genotypes of their putative parents (i.e. grandparents of the larval families) using CERVUS 3.0 (Kalinowski et al., 2007). The wild-type broodstock used as the foundation population for the breeding program was used as the base population for simulations to determine critical thresholds for parentage analyses (Kalinowski et al., 2007). The proportion of loci typed was set to 1.00 and the genotyping error rate set at the default value of 1%. Determination of parentage was based on 95% confidence levels for assignment to the most likely candidate parent pair.

Larval families

Eggs and sperm were removed directly from the gonads of genotyped, gravid *C. gigas*. To avoid cross-contamination, clean Pasteur pipettes were used to obtain gametes from each adult. Eggs were placed in filtered seawater for enumeration. Aliquots of sperm from each male were added to separate 1.5 ml micro-centrifuge tubes and kept 'dry' (no seawater added) at 4°C. Once the number of eggs was known, seawater was added to the sperm and approximately 1 ml of this sperm suspension was added to 1 liter of seawater containing eggs. Fertilization success was confirmed by microscopic observation of first polar body formation (~20 min).

Table 1 lists the genotyped males and females selected for crosses to generate 21 larval families. Of the 21 larval families produced, 10 represented first-generation (G_1) families from sibling parents and the remaining 11 families represented G_0 families from unrelated parents (Table 1). For each sire×dam cross, the combination of each letter and number designates an individual male or female. Depending upon the fecundity (and sperm and egg quality) of each individual male and female used for crosses, some larval families were produced by using the same genotyped parent or sibling adult from the same parental line. This is indicated with repetition of the same letter and number, when the same individual adult was used to generate two families, producing half-sibling offspring larvae. For example, larval family 1 was produced by crossing male A and female B in a sire×dam cross. Male A was also used to produce half-sibling offspring for larval family 4, by crossing male A with a different female, female E. Hence, larval families 1 and 4 have a relatedness (co-ancestry) of 0.25. Larval families 2 and 3 have a relatedness of 0.375 because females D.1 and D.2 were siblings and were crossed with the same parent, male C. Larval families 1–4 were all generation G_0. Larval families 6 and 15 are examples of generation G_1 larval families, produced

Journal of Experimental Biology (2022) 225, jeb244518. doi:10.1242/jeb.244518

Table 1. Genotyped male and female broodstock of *Crassostrea gigas* crossed to generate larval families 1–21

Family no.	Generation	Male	Female
1	G_0	A	B
2	G_0	C	D.1
3	G_0	C	D.2
4	G_0	A	E
5	G_1	F.1	F.2
6	G_1	G.1	G.2
7	G_1	F.3	F.2
8	G_1	H.1	H.2
9	G_0	I	J
10	G_0	K	L
11	G_0	M.1	N
12	G_1	O.1	O.2
13	G_1	M.2	M.3
14	G_1	H.1	H.3
15	G_1	G.3	G.4
16	G_0	O.1	P
17	G_1	Q.1	Q.2
18	G_0	R	S
19	G_0	T	U
20	G_1	Q.3	Q.2
21	G_0	V	W

Each letter and number combination designates an individual sire×dam cross. Generation G_0 represents a larval family produced from unrelated adults. Generation G_1 represents a larval family obtained from a full-sibling mating.

from four separate parents that were bred from the same pedigreed line (larval family 6 from G.1×G.2; larval family 15 from G.3×G.4). See Lynch and Walsh (1998) for calculations of genetic coefficients for relatedness.

Fertilized eggs from each of the 21 sire×dam crosses were stocked at an initial number of 10 eggs ml^{-1} in a series of 200 l culture vessels. All larval families were reared at 25°C in a custom-designed, large-scale culturing facility at the Wrigley Marine Science Center (University of Southern California) located on Santa Catalina Island. Seawater used to culture all larval families was obtained directly from the Pacific Ocean surrounding Catalina Island. Ambient seawater was filtered (0.2 µm pore -size) and heated with inert (titanium) heat exchangers to the desired temperatures. During larval rearing, seawater in each culture vessel was replaced every 2 days by removing larvae from culture vessels and gently washing them on size-appropriate mesh sieves with filtered seawater.

During experiments, temperature was measured every 30 min (HOBO data logger U12, Onset Computer Corp., Bourne, MA, USA) in selected 200 l culture vessels. A total of over 2400 such temperature measurements were made, yielding a mean (±s.e.m.) temperature of 24.9±0.01°C. At 25°C – a routine temperature used to grow larvae of *C. gigas* – the first larval feeding stage (D-hinge veliger larva) developed by 2 days. The alga *Tisochrysis lutea* (*T-ISO*, CCMP1324, National Center for Marine Algae and Microbiota, Bigelow, ME, USA) (Helm and Bourne, 2004) was added to each larval culture vessel at 30,000 cells ml^{-1}. Algal ration was later increased to 50,000 cells ml^{-1} as larvae grew (per standard culturing protocols for larvae of *C. gigas*, as described by Breese and Malouf, 1975; Helm and Bourne, 2004).

Larval growth and survivorship

Growth and survivorship of individuals from each larval family were evaluated throughout experiments. Survivorship was based on enumerations of known aliquots of larvae, re-suspended in a volume of 200–500 ml (dependent on the number of larvae collected from each culture vessel). Replicate (at least 3) enumerations of larvae were completed for each larval family to yield a coefficient of variation of less than 10%. Known numbers of larvae were then placed in a range of experimental containers used for the measurement of respiration, amino acid transport and protein synthesis rates. Growth rate was measured from the shell lengths of larvae over time. Larvae were photographed at 40× magnification in Sedgewick Rafter counting chambers, with 1–2 drops of ethanol added for immobilization. At least 50 larvae at specific time points selected within each culture vessel were measured for length, using digital assay software for shell length analyses (ImageJ, National Institutes of Health, Bethesda, MD, USA). A total of approximately 5000 larval sizes were measured during the course of the larval culturing required for these experiments. Protein content of selected larval families was also assayed (Bradford, 1976; as modified by Jaeckle and Manahan, 1989).

Respiration rate and Q_{10} values

For analysis of the temperature sensitivity (Q_{10} value) of respiration, a total of 41 Q_{10} values were measured using a total of 1600 individual micro-respiration chambers. To obtain the respiration rate, the amount of oxygen in each chamber was measured at least 4 times during a time course experiment (Fig. 1A–C). Respiration rates of larvae were measured as oxygen consumption over time, using optode technology (Witrox-1 Oxygen Meter, Loligo Systems, Viborg, Denmark). This technology was previously calibrated and determined to be consistent with respirometry measurements made with polarographic oxygen sensors for *C. gigas* larvae (Pan et al., 2021). A known number of larvae (between 250 and 400, depending on size) was placed in a series of replicate glass, sealed micro-biological oxygen demand respiration chambers. Each respiration chamber (up to 40 different respiration chambers were used for a given assay) was individually calibrated for volume (between 400 and 700 µl). Each respiration chamber contained an internal 2 mm diameter sensor spot (Presens, Regensburg, Germany), to which a fiber optic cable was non-invasively and manually held near the sensor spot for each measurement of oxygen. This permitted a series of time course assays for the rate of oxygen depletion by larvae in each individual respiration chamber. For each larval family, oxygen consumption was measured with at least seven replicate chambers over the range of selected temperatures (Fig. 1D–F: 14–28°C) used to determine Q_{10} value. This temperature range was chosen as it is representative of the natural environments where larvae of *C. gigas* are known to be present in the water column (Pacific Northwest: Quayle, 1988).

Prior to the start of each temperature assay, larvae were pre-incubated for 30 min at each temperature treatment tested. Previous experiments using chronic (days to weeks) and acute (minutes to hours) exposures of *C. gigas* larvae to different temperatures showed that similar values of respiration Q_{10} were obtained with either treatment (Pan et al., 2021). For each assay, each respiration chamber was measured 4–5 times during a time course assay of approximately 3 h (assay time depended on larval size and oxygen depletion). Control chambers which contained no larvae, just filtered (0.2 µm pore size) seawater, were included for each measurement of respiration at all temperatures tested. Linear regressions of the decrease in oxygen over time – corrected for volume of each respiration chamber and the number of larvae in each respiration chamber – were used to calculate the respiration rate as pmol O_2 $larva^{-1}$ h^{-1}. This process was repeated for each of the four experimental temperatures tested (Fig. 1D–F). Assays for each of these temperature treatments were used to calculate a Q_{10} value for respiration, using a standard equation for Q_{10} (Schmidt-Nielsen, 1997), where the rate (R) and the temperature (T) correspond to two

Journal of Experimental Biology (2022) 225, jeb244518. doi:10.1242/jeb.244518

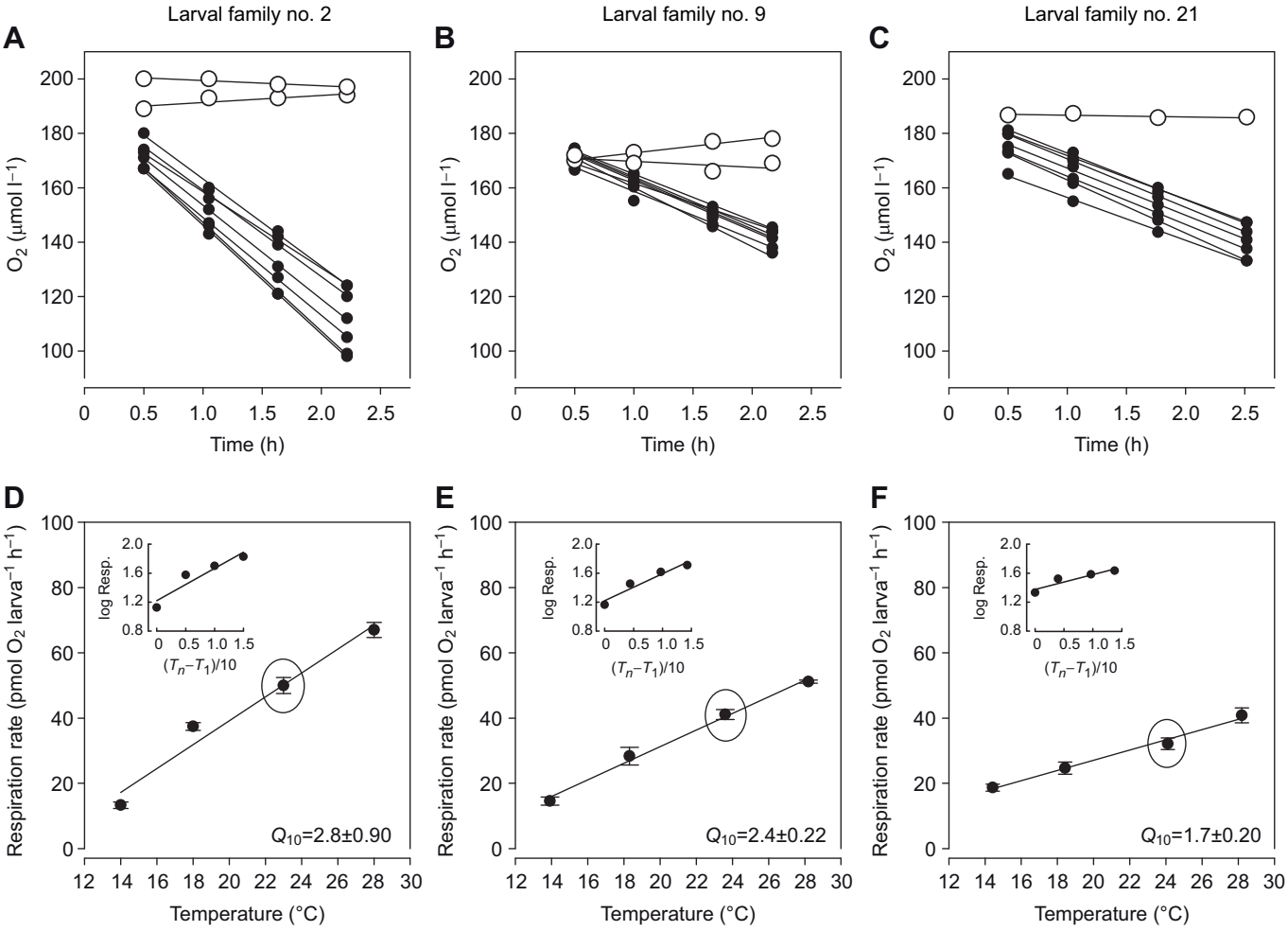

Fig. 1. Time course of oxygen depletion by larvae of *Crassostrea gigas*. (A–C) Time course of oxygen depletion in the respiration chamber for larval family 2 (400 larvae per chamber), (B) 9 and (C) 21 (both 250 larvae per chamber). Filled symbols represent respiration chambers with larvae present (experimental); open symbols represent chambers with no larvae present (controls). (D–F) Respiration rates measured at four temperatures for calculation of Q_{10} values for larval family 2 (D), 9 (E) and 21 (F). Circled data points in D–F were calculated from the replicate set of measurements for the corresponding families shown in A–C. *N*=7 replicate respiration chambers for each data point; means±1 s.e.m. Inset graphs in D–F show the actual log plots used to calculate Q_{10} values (given ±s.e.).

separate respiration rates (R_1 and R_2) measured at two different temperatures (T_1 and T_2):

$$Q_{10} = \left(\frac{R_2}{R_1}\right)^{\frac{10}{T_2 - T_1}}. \quad (1)$$

This equation was converted to the log of the respiration rate, in relation to the temperature increment of $(T_n - T_1)/10$, to allow the calculation of Q_{10} values at four temperatures ($Q_{10}=10^{\text{slope}}$). For this calculation for a given larval family at a given size, data included each of the four different temperature assays, each measured with 7–10 respiration chambers. The standard error for each Q_{10} value is a propagated error corrected for the standard error of the slope from the log equation (from Taylor, 1982: ln10×Q_{10} value×s.e. of slope). These sets of respiration measurements were repeated for larvae of different sizes for each of the 21 families assayed (e.g. comparison of larval family 2 in Fig. 1D, larval family 9 in Fig. 1E, larval family 21 in Fig. 1F). Additionally, for some larval families, larvae were size fractionated (retained on mesh screens) to be of similar size, but of different age (as a result of differential growth rates of sibling larvae within a family).

ANCOVA linear regressions were used to test whether a measured Q_{10} value for respiration within a larval family changed with growth, over a range of developmental sizes spanning 80 µm (newly formed veliger larva) to 280 µm (nearing metamorphic competence) in shell length (size range shown in Fig. 2). ANOVA with *post hoc* Tukey tests were used to test for differences in respiration Q_{10} values among the 21 larval families. ANCOVA was used to test for differences between G_0 and G_1 larval families. For statistical tests, values of total corrected degrees of freedom are provided with the *F*-statistic.

Protein synthesis rate and Q_{10} values

For analysis of the temperature sensitivity of protein synthesis, two larval families were studied in detail (families 9 and 21). These larval families were chosen because family 9 had an average respiration Q_{10} of 2.3, in contrast to family 21 which had a lower respiration Q_{10} of 1.6 (Table 2).

Amino acid transport rate

Amino acid transport rates were determined by *in vivo* time course assays with [^{14}C]glycine as the substrate added to seawater.

Journal of Experimental Biology (2022) 225, jeb244518. doi:10.1242/jeb.244518

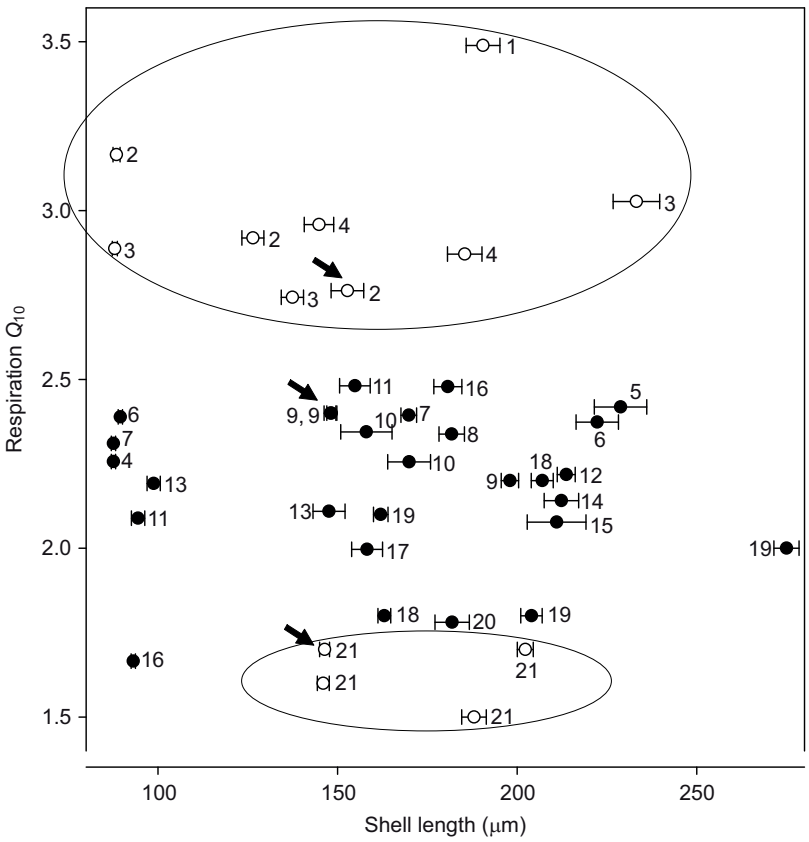

Fig. 2. Respiration Q_{10} values for different-sized *C. gigas* larvae measured in 21 larval families. Family number is indicated by each data point. Horizontal error bars are for shell length (±1 s.e.m.). Errors for Q_{10} values are given in Table 2. Upper ellipse represents the high Q_{10} values of larval families 1–4 (open symbols within ellipse), except for one value for family 4 (Q_{10} 2.3, Table 2). Lower ellipse represents the low Q_{10} values of family 21 (open symbols within ellipse). Each clustering of larval families is based on ANOVA and *post hoc* Tukey test (see Materials and Methods, 'Respiration rate and Q_{10} values'). Arrows placed by larval families 2, 9 and 21 indicate the same-sized larvae of those three families that had different Q_{10} respiration values shown in Fig. 1. Filled symbols indicate larval families not included in the upper and lower ellipses.

Previously selected for studies of *C. gigas* larvae (Lee et al., 2016; Pan et al., 2018, 2021), [^{14}C]glycine was chosen as the radioisotope tracer of protein synthesis based on the composition of the intracellular free amino acid pool of *C. gigas*. Each time course assay was conducted in duplicate 20 ml sealed glass vials, each containing 10,000 larvae in 10 ml of filtered seawater. An addition of 74 kBq of [^{14}C]glycine (Perkin Elmer, Boston, MA, USA) was supplemented with non-radioactive glycine (Sigma-Aldrich, St Louis, MO, USA) to provide a total glycine concentration of 10 μmol l^{-1} in seawater prior to the start of each transport assay. A 15 μl aliquot of seawater was taken at the start of each assay to quantify the specific activity of [^{14}C]glycine in each experimental assay vial. The specific activity was used to correct the amount of [^{14}C]glycine to total glycine transported from seawater by larvae. A series of six 1 ml samples (each containing 1000 larvae) was removed from each replicate vial every 8 min during a 48-min time course assay. Samples were transferred onto an 8 μm pore-size (Nuclepore, GE Healthcare, Pittsburgh, PA, USA) membrane filter and, under gentle vacuum, the excess radioactivity in seawater was removed with additional washes of filtered seawater. Filters holding larvae were then placed in 1.5 ml micro-centrifuge tubes and frozen at −80°C until further processing.

Table 2. Larval families 1–21 ranked by mean respiration Q_{10} value

Family no.	Mean Q_{10} value	i	ii	iii	iv
1	3.5	3.5±0.48			
2	2.9	3.2±1.77	2.9±0.33	2.8±0.90	
3	2.9	2.9±0.53	2.7±0.68	3.0±0.76	
4	2.7	2.3±0.16	3.0±0.21	2.9±0.67	
5	2.4	2.4±0.39			
6	2.4	2.4±0.22	2.4±0.33		
7	2.4	2.3±0.05	2.4±0.06		
8	2.3	2.3±0.26			
9	2.3	2.4±0.22	2.2±0.05	2.4±0.72	
10	2.3	2.3±0.26	2.3±0.32		
11	2.3	2.1±1.16	2.5±0.29		
12	2.2	2.2±0.20			
13	2.2	2.2±0.61	2.1±0.10		
14	2.1	2.1±0.39			
15	2.1	2.1±0.19			
16	2.1	1.7±0.31	2.5±0.35		
17	2.0	2.0±0.14			
18	2.0	1.8±0.12	2.2±0.10		
19	2.0	2.1±0.10	1.8±0.08	2.0±0.32	
20	1.8	1.8±0.08			
21	1.6	1.6±0.18	1.5±0.07	1.7±0.20	1.7±0.08
Overall mean	2.3±0.1				

Columns labeled i–iv represent measurements on larvae of different size or age. Specific sizes within a larval family are shown in Fig. 2. Data are calculated Q_{10} value ±1 s.e. of slope (see Materials and Methods).

Frozen larvae were processed by adding 400 μl of deionized water (Nanopure, Barnstead™ Nanopure Bioresearch Deionization System, Dubuque, IA, USA) to each sample tube kept on ice, followed by homogenization with a Vibra-cell ultrasonic processor fitted with a 3 mm micro-probe (Sonics & Materials, Inc., Newton, CT, USA) for two 15 s intervals. A 15 μl aliquot of the homogenate was placed directly into a scintillation vial containing liquid scintillation counting fluid (Ultima Gold™, Perkin Elmer). Total radioactivity was counted with appropriate quench correction (Beckman Coulter Liquid Scintillation Counter, Model 6500). The rate of glycine transport by larvae (Fig. 3A) was calculated from the slope of the accumulation of [^{14}C]glycine over time, corrected for the starting specific activity of [^{14}C]glycine in each assay vial and for the number of larvae per sample. Duplicate time course

Journal of Experimental Biology (2022) 225, jeb244518. doi:10.1242/jeb.244518

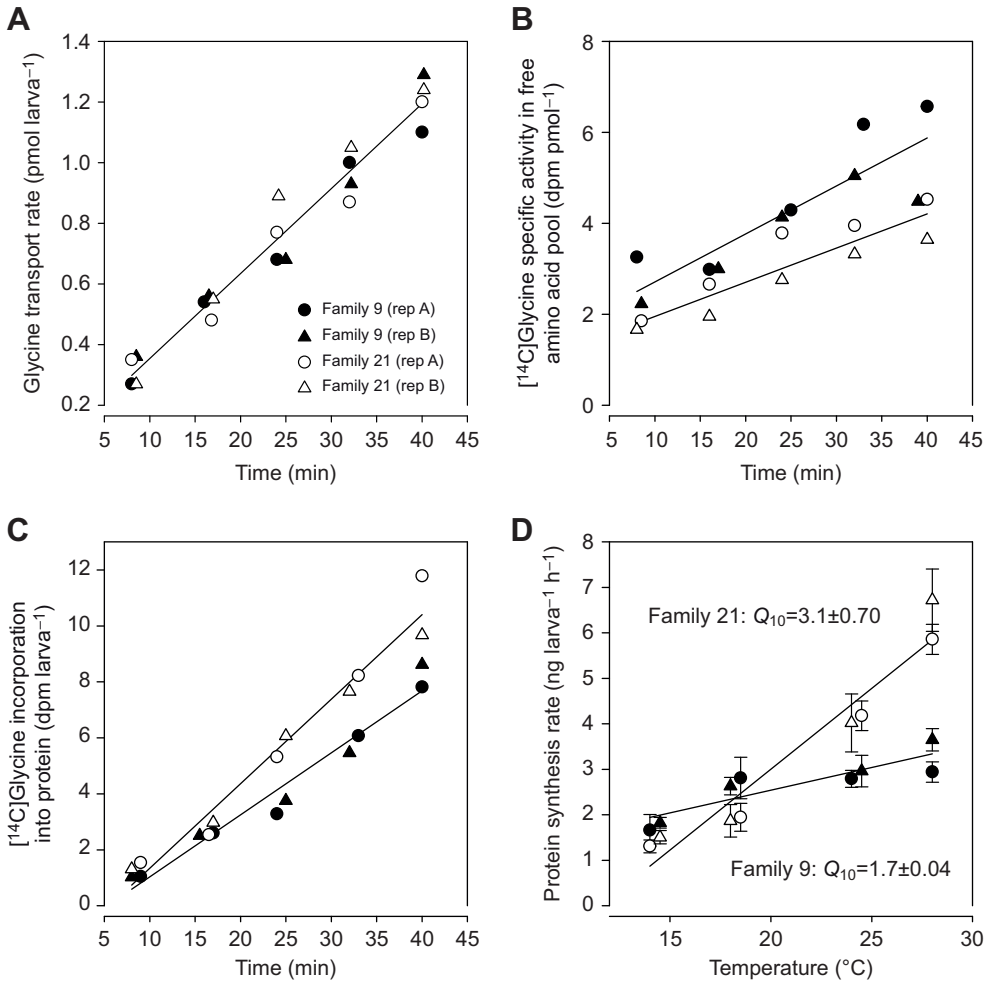

Fig. 3. Protein synthesis by similar-sized (147 µm) *C. gigas* larvae from larval families 9 and 21. (A) Glycine transport rate measured at 28°C in duplicate assays (rep A and B) for each larval family. A single regression line is shown, calculated for all data points (see ANOVA, Results, 'Protein synthesis'). (B) Change in [^{14}C]glycine specific activity in the intracellular free amino acid pool of larvae. (C) Incorporation of [^{14}C]glycine into the trichloroacetic acid (TCA)-precipitable protein fraction of larvae. (D) Protein synthesis rate measured at four temperatures for calculation of Q_{10} values. Error bars represent s.e. of the slope.

assays at each of four temperatures were used to calculate the Q_{10} value for glycine transport. An ANCOVA was used to compare the Q_{10} values for glycine transport within and between families. This analysis was used to compare the effect of temperature on the acquisition of substrate (amino acid transport) with the metabolism of substrate (amino acid incorporation into protein).

Protein synthesis rate

Protein synthesis rates were calculated from data obtained during the corresponding *in vivo* time course assays of the transport rate by larvae of [^{14}C]glycine (Fig. 3A). From each of the 400 µl larval homogenate samples prepared from each time point of a time course assay as described above, a 300 µl aliquot was used to determine the amount of [^{14}C]glycine that was incorporated into protein. An additional 42 µl of homogenate was used to determine the intracellular specific activity of [^{14}C]glycine in the extracted free amino acid pool of larvae (Fig. 3B). The rate of protein synthesis was calculated by combining (1) the rate of incorporation of [^{14}C]glycine into the trichloroacetic acid (TCA)-precipitable protein fraction (Fig. 3C) with (2) the rate of change in the intracellular specific activity of [^{14}C]glycine in the free amino acid pool (Fig. 3B).

The intracellular specific activity of [^{14}C]glycine in the free amino acid pool of larvae was determined by high-performance liquid chromatography. For extraction of the free amino acid pool from larval tissues, a 42 µl aliquot of the original (400 µl) larval homogenate (as prepared above) was combined with 100 µl chromatographic-grade 100% ethanol to yield a final concentration of 70%. Samples were incubated at 4°C for at least 24 h and then centrifuged for 5 min at 12,000 rpm prior to chromatographic analysis (for further details see Lee et al., 2016). In brief, the chromatographic separation and quantification of the amount (moles) of glycine in each sample (100 µl injection chromatographic sample loop) was combined with quantification of the amount of radioactivity in the glycine chromatographic peak (collected by fraction collector; Model FC 203B, Gilson Inc., Middleton, WI, USA). These data were used to calculate the rate of change of the intracellular specific activity of [^{14}C]glycine in the free amino acid pool (Fig. 3B), required for calculations of absolute rates of protein synthesis. These methods were used to calculate protein synthesis rates for different larval families, with the full suite of chromatographic and radiochemical measurements repeated at each different temperature.

The amount of [^{14}C]glycine incorporated into protein was measured by taking 300 µl of the larval homogenate with an equal amount of 10% trichloroacetic acid added to yield a final concentration of 5%. After a 30 min incubation at 4°C, homogenates were vortexed and placed on a GF/C glass microfiber filter (Whatman, Tisch Scientific, North Bend, OH, USA) to retain TCA-precipitable protein. Under gentle vacuum, the [^{14}C]glycine not incorporated into the TCA-precipitable protein fraction was removed by additional washes with 5% TCA and methanol. Each filter containing the protein precipitate was transferred into a liquid scintillation vial for subsequent determination of the amount of radioactivity. The slope of the increase with time of the rate of

Journal of Experimental Biology (2022) 225, jeb244518. doi:10.1242/jeb.244518

incorporation of [^{14}C]glycine into protein was measured in duplicate assays for a given larval family at each temperature tested (Fig. 3C).

The rate of protein synthesis was calculated as:

$$\mathrm{d}/\mathrm{d}t(S_\mathrm{p} \div S_\mathrm{faa}) \times 126.6 \div 12, \quad (2)$$

where S_p is the amount of radioactivity in the protein fraction of larvae; S_faa is the amount of radioactivity in the free amino acid pool of larvae; t is each sample point of a time course assay; 126.6 represents the measured grams per mole of the mole-percent corrected molecular mass of all amino acids comprising the whole-body protein content of larvae; and 12 is the percentage of glycine in the amino acid composition of hydrolyzed, whole-body protein of *C. gigas* larvae (from Lee et al., 2016). To calculate a Q_{10} value for the rate of protein synthesis, this set of analytical and calculation steps was repeated at each of four different temperatures (Fig. 3D), with the linear regression measured at each temperature used for the duplicate determinations of the protein synthesis rate (represented in Fig. 3D as a single data point with s.e. of the slope, where each data point represents N=5). ANCOVA (with appropriate confirmation of normality) was used to compare Q_{10} values within and among different larval families.

Allocation of energy to support the cost of protein synthesis with rising temperature

The rates of respiration (moles of oxygen) and protein synthesis (grams) were converted to energy equivalents (joules: Gnaiger, 1983; Lee et al., 2016). This conversion allowed the calculation of energy allocation strategies used by different larval families to support increased protein synthesis rates in response to increased temperature.

Protein and lipid are the major biochemical components in *C. gigas* larvae (Moran and Manahan, 2004; Pan et al., 2018). A value of 484 kJ mol^{-1} O_2 was used to convert moles of oxygen to joules (mean value of 441 kJ mol^{-1} O_2 for lipid; 527 kJ mol^{-1} O_2 for protein). For physiological energetics, these oxyenthalpic equivalents for combustion of catabolized biomass are routinely used (Gnaiger, 1983). An additional justification for the use of 484 kJ mol^{-1} O_2 is that the measured calorimetric–respirometric ratio for *C. gigas* larvae under normoxic conditions is 478 kJ mol^{-1} O_2 (Hand, 1999; see also Haws et al., 1993), a value that is within 1% of the value (484 kJ mol^{-1} O_2) used here to calculate energy allocation. For protein synthesis in *C. gigas* larvae, the energy to synthesize a unit mass of protein is 2.1±0.2 J mg^{-1} protein synthesized (mean±s.e.m.) (Lee et al., 2016). Of importance for calculating energy allocation models in the current study is that this cost of protein synthesis is independent of temperature, growth rate (size) and genotype.

RESULTS

Larval condition and quality

The project goal was attained by generating multiple larval families of *Crassostrea gigas* for physiological analysis. To ensure that each larval family was distinct (single sire×dam crosses), genetic relatedness was confirmed by genotyping each set of parents (Table 1). The larvae in all 21 families grew under the culturing conditions utilized for food ration and 25°C rearing temperature. Of the fertilized eggs that developed at 25°C to the first larval feeding stage at day 2 (57 million D-hinge veliger larvae across all 21 larval families tested), a mean of 45% survived to day 11. This value compares well to the typical survival rate during the larval stage of oysters of approximately 50% (Helm and Bourne, 2004). Additionally, larvae from 17 of the 21 families underwent successful metamorphosis to the early juvenile stages, indicating the general viability and health of the larvae studied.

Respiration

Measurement of oxygen consumption

Fig. 1A–C illustrates an example of the level of replication used to measure rates of oxygen consumption of larvae from three different families (families 2, 9 and 21). The primary respiration data obtained for these three larval families span a broad range of Q_{10} values and illustrate the size independence of respiration Q_{10} values (Fig. 2). In addition, data from larval families 9 and 21 were used to calculate the model illustrated in Fig. 4, highlighting the differential allocation of energy to protein synthesis with rising temperature. Respiration rates of larvae were measured in a series of seven independent micro-biological oxygen demand respiration chambers. Also illustrated in Fig. 1A–C are blank control measurements, showing the insignificant depletion of oxygen in respiration chambers when no larvae were present (filtered seawater only) (e.g. Fig. 1A: combined ANOVA of the two control regressions, P=0.9). All of the independent rate measurements of respiration (from each respiration chamber) shown in Fig. 1A–C were obtained at a single temperature. Larvae used in these measurements from each of these three different families were of similar size (mean±s.e.m., family 2: 153±4.5 µm, family 9: 148±1.3 µm, family 21: 146±1.4 µm). By ANOVA, these three larval sizes were not significantly different ($F_{2,153}$=2.34, P=0.1). Those replicate measurements of respiration within a family were pooled and graphed as a single point (circled in Fig. 1D–F) for a specific temperature (with corresponding measurement error). These analyses of respiration rates were repeated at temperatures of 14, 18 and 28°C for each larval family (Fig. 1D–F).

Rates of oxygen consumption were then used to calculate Q_{10} values for the respiration rates for each larval family. Values of Q_{10} were calculated from the log value of the respiration rate at each of the four temperatures assayed. For instance, larval family 2 (Fig. 1D) had a high Q_{10} value (±s.e.) of 2.8±0.90 (N=28, R^2=0.90), larval family 9 (Fig. 1E) had an intermediate Q_{10} value of 2.4±0.22 (N=28, R^2=0.99) and larval family 21 (Fig. 1F) had the lowest Q_{10} value of 1.7±0.20 (N=28, R^2=0.99). ANCOVA for these three Q_{10} values showed significant differences ($F_{2,78}$=15.32, P<0.0001). Hence, there was a significant difference (Tukey's comparison) between these three larval families with respect to temperature, with family 2 having a greater sensitivity to temperature increase than family 9, and both families having a greater sensitivity than family 21.

Q_{10} values for multiple larval families

Combined for all 21 families studied, a total of 41 Q_{10} values were measured for larvae reared to different sizes (shell length range from 80 to 280 µm). This experimental analysis was designed to address the question of whether larval growth and size alter the physiological response to temperature within specific larval families. As detailed below, statistical analysis revealed that larval size did not change the Q_{10} value for respiration within a family. Importantly, there were significant differences (statistical values below) among larval families with respect to the response to temperature.

The 21 larval families that were assayed during the course of this study were ranked from the highest Q_{10} value of 3.5 for larval family 1 to the lowest Q_{10} of 1.6 for larval family 21 (Table 2). For the latter

Journal of Experimental Biology (2022) 225, jeb244518. doi:10.1242/jeb.244518

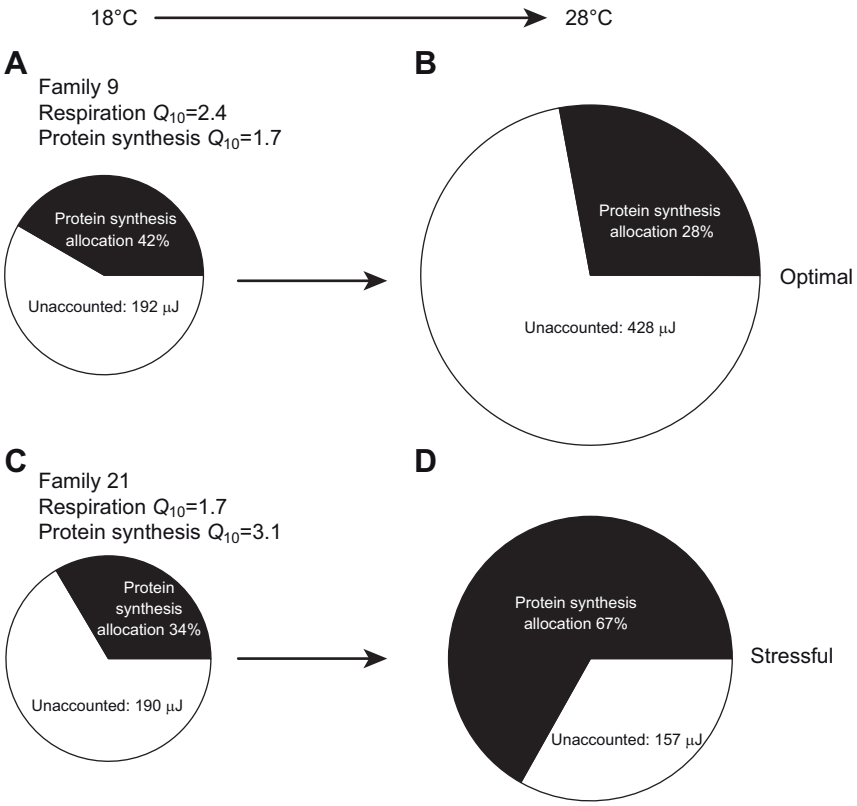

Fig. 4. Energy allocation to protein synthesis with increasing temperature for similar-sized (147 µm) *C. gigas* larvae from larval families 9 and 21. Total area of the pie charts (family 9: A 329 µJ, B 594 µJ; family 21: C 286 µJ, D 476 µJ) represents the conversion from moles of respiratory O_2 to joules. Areas shaded black represent allocation of energy to protein synthesis (for details of oxyenthalpic equivalents and cost of protein synthesis, see Materials and Methods, 'Allocation of energy to support the cost of protein synthesis with rising temperature'). Energy not accounted for by protein synthesis is labelled 'unaccounted'. (A,B) Change in percentage energy allocation to protein synthesis for a temperature change from 18°C to 28°C for larval family 9. (C,D) Change in percentage energy allocation to protein synthesis for a temperature change from 18°C to 28°C for larval family 21.

family, for instance, four different larval sizes were assayed for Q_{10} respiration values (mean±s.e.m. larval shell length columns i–iv, respectively: 188±3.4, 146±1.6, 146±1.4 and 202±2.2 µm). The two mean values of 146 µm for larval family 21 represent larvae of similar size, but differing in age by 2 days (size-fractioned, see Materials and Methods, 'Respiration rate and Q_{10} values'). Complete details of the range of larval sizes tested within each larval family are given in Fig. 2. ANOVA of all data for the 21 larval families and all larval sizes assayed revealed that size did not change the Q_{10} value within a family ($F_{1,39}$=0.56, P=0.46). There was, however, a significant difference for Q_{10} values among families ($F_{20,40}$=7.03, P<0.001), with larval family accounting for 87% of the variance. This level of difference explained by family was calculated based on the ratio of the sum of squared deviation from the mean for the family effect (7.1) to the total sum of squared variance (8.2).

Tukey's pairwise comparison (α=0.05) following ANOVA identified the larval families with the highest and lowest response of respiration rate (Q_{10} values) to temperature. This clustering of families is shown in Fig. 2. Larval families 1–4 (Fig. 2, upper ellipse) had the greatest sensitivity to temperature, compared with all other families. Each of the respective Q_{10} values for these four larval families – representing a wide range of different larval sizes – was by 95% confidence interval not different from a Q_{10} of 3.0 (calculated from the s.e. of the slope regression analysis for each Q_{10} value, Table 2). In contrast, larval family 21 had the lowest respiration Q_{10} of 1.6 (Table 2), illustrated as the lower ellipse in Fig. 2. The other 16 larval families (families 5–20; see Fig. 2) had Q_{10} values for respiration that were less than the Q_{10} value of 3.0 for larval families 1–4 and were greater than the Q_{10} value of 1.6 for larval family 21. The detailed oxygen consumption data for larvae of the same size in families 2, 9 and 21 (Fig. 1), with different Q_{10} values, are indicated by arrows on Fig. 2. An ANCOVA regression of 41 respiration Q_{10} values, for all 21 families, and 11 G_0 and 10 G_1 generations revealed a significant effect of generation ($F_{1,40}$=8.05, P=0.007). There was a marginally significant interaction between family and generation ($F_{1,40}$=4.5, P=0.04) (least square mean±s.e.m. Q_{10} value: G_0=2.4±0.04, G_1=2.2±0.06; P=0.04).

In summary, Q_{10} values for respiration within a family did not change during larval growth, as at any given size the Q_{10} values were similar. Significant differences in Q_{10} values among families and between generations were evident, which has important implications for biological variation in response to temperature (Figs 1 and 2, Table 2).

To address a possible relationship between respiration rates for larval families that were (or were not) successful in reaching metamorphosis as late-stage larvae, respiration rates were compared for larval families that completed metamorphosis with those larval families that did not complete metamorphosis. To correct for size-dependent effects in respiration, larvae of a similar size were compared (see size range in Fig. 2 for larvae of approximately 150 µm in shell length: 137–163 µm). This dataset contains a total of 11 larval families for which respiration rates were measured for larvae of ∼150 µm. Of these 11 larval families, eight were successful in metamorphosing to the early juvenile stage (larval families 2, 3, 10, 11, 17, 18, 19, 21) and three larval families were not (larval families 4, 9, 13). A comparison of respiration rates measured at the rearing temperature of 25°C shows that larvae from families that completed metamorphosis had similar (t-test, P=0.121) respiration rates (mean±s.e.m. 68.7±5.9 pmol O_2 h^{-1}) to larvae that did not complete metamorphosis (51.0±6.8 pmol O_2 h^{-1}), i.e. there was no relationship between larval respiration and successful metamorphosis.

Protein synthesis

The change in the rate of protein synthesis with increasing temperature was measured for larval families 9 and 21 (Fig. 3).

Journal of Experimental Biology (2022) 225, jeb244518. doi:10.1242/jeb.244518

Family 9 was chosen because it had an average Q_{10} value of 2.3, the same as the overall mean Q_{10} of 2.3±0.1 for all 21 families (Table 2). Family 21 was chosen because it had the lowest Q_{10} value for respiration (Q_{10} of 1.6, from Table 2). Notably, larvae from each of these two families had similar rates of glycine transport from seawater, averaging 1.7±0.06 pmol glycine larva^{-1} h^{-1} (mean±s.e.m.) (Fig. 3A, at 28°C). By ANCOVA, this transport rate of [^{14}C]glycine from seawater by larvae was similar for the duplicate assays within a larval family and between the two families (ANCOVA $F_{1,16}$=0.24, P=0.6). The rates of protein synthesis, however, differed significantly (statistical values below) between these two larval families. Fig. 3B,C illustrates the measurement steps used to determine the rate of protein synthesis for larval families 9 and 21. Notably, the intracellular specific activity differed for the transported [^{14}C]glycine in the free amino acid pools of larvae for these two families (Fig. 3B). Replicate assays within a family did not differ statistically (family 9, ANCOVA slope: $F_{1,6}$=1.49, P=0.3; family 21, ANCOVA slope: $F_{1,6}$=1.63, P=0.3). Within each larval family, a single regression line is shown calculated from the pooled data from the two time course assays. There was no difference in slope between the two regression lines (ANCOVA $F_{1,16}$=1.25, P=0.3), but there was a significant difference in the intercepts of the regressions between families 9 and 21 (ANCOVA $F_{1,17}$=18.51, P=0.0005). The difference in intercept, and not in slope, indicated a difference in the amount (moles) of glycine in the free amino acid pool of larvae from families 9 and 21. For example at 28°C, family 9 had an average of 4.4±0.2 pmol glycine larva^{-1}, which was significantly lower than that of family 21, which averaged 6.3±0.2 pmol glycine larva^{-1} (ANOVA $F_{1,18}$=31.1, P<0.0001). Hence, the higher specific activity of glycine in the free amino acid pool measured for family 9 (Fig. 3B) is attributable to a smaller amount of total glycine in the pool. As the same amount of [^{14}C]glycine was transported by larvae from each family (Fig. 3A), that radioactivity was differentially diluted by the amount of glycine in the free amino acid pool of larval families 9 and 21. This is reflected in the higher intracellular specific activity of [^{14}C]glycine in family 9 (the ratio of [^{14}C]glycine to total glycine).

Additionally, larval families 9 and 21 showed differences in the rate of incorporation of [^{14}C]glycine into protein (Fig. 3C). Replicate assays within a family did not differ statistically (family 9, ANCOVA slope: $F_{1,6}$=0.15, P=0.7; family 21 ANCOVA slope $F_{1,6}$=2.57, P=0.2); those data were pooled into a single regression for each larval family. Larvae from family 21 had a significantly faster rate of incorporation of [^{14}C]glycine into protein than larvae from family 9 (ANCOVA $F_{1,16}$=9.50, P=0.007). Similar sets of assays were conducted over the temperature range shown in Fig. 3D. The log value of the average protein synthesis rate at each temperature was used to calculate the Q_{10} value. An ANOVA regression gives the Q_{10} value as 10^{slope} and was 1.7±0.04 (Q_{10} ±s.e.) for the rate of protein synthesis for larvae from family 9, and 3.1±0.7 for the rate of protein synthesis for larvae from family 21. Larvae from family 21 had a significantly higher temperature sensitivity (Q_{10} value) for protein synthesis rate than larvae from family 9 (ANCOVA slope $F_{1,12}$=42.95, P<0.0001).

Differences in Q_{10} values for respiration and protein synthesis in specific larval families

The analysis of differences in Q_{10} values for respiration (Table 2) highlighted overall significant differences in temperature response between larval family 9 (Q_{10} of 2.3) and 21 (Q_{10} of 1.6). These two larval families with different responses of respiration to temperature also had different temperature responses for rates of protein synthesis. This comparison for protein synthesis of the two families was based on larvae of similar size, at 147 µm (mean±s.e.m. family 9: 148±1.3 µm; family 21: 146±1.4 µm). By ANOVA, larval sizes between these two families were not different: $F_{1,107}$=1.02, P=0.3. Also, these same-sized larvae from family 9 and 21 had a similar protein content (mean±s.e.m. family 9: 64.9±4.2 ng protein larva^{-1}; family 21: 67.0±2.1 ng protein larva^{-1}). Larval family 9 at this size fraction had a greater respiration Q_{10} of 2.4±0.22, compared with a Q_{10} of 1.7±0.20 for family 21 (by ANCOVA, these Q_{10} values were different: $F_{1,50}$=5.56, P=0.02). Strikingly, the reverse pattern was measured for the temperature sensitivity of protein synthesis (Fig. 3D), where larval family 21 had a greater Q_{10} value of 3.1±0.7 and family 9 the lower Q_{10} of 1.7±0.04 (by ANCOVA these Q_{10} values were different: $F_{1,12}$=42.79, P<0.0001).

In summary, a physiological difference was identified between larval families 9 and 21 with respect to the alternation of thermal sensitivity for the supply of energy (respiration) and demand for energy (protein synthesis). This difference in protein synthesis was not driven by acquisition of substrate, because the rate of amino acid transport from seawater was equivalent between larval families at any given temperature tested (e.g. at 28°C, Fig. 3A: ANCOVA, $F_{1,16}$=0.24, P=0.6). Larval families 9 and 21 had a similar Q_{10} value for glycine transport of 1.8±0.2.

Differing energy allocation strategies for larval families in response to temperature change

The different Q_{10} values for respiration and protein synthesis for families 9 and 21 have substantial consequences for the supply and demand of energy allocation and availability (illustrated in Fig. 4). In this analysis, the rates of respiration (Fig. 1E,F) and protein synthesis (Fig. 3D) were converted to energy equivalents to compare energy supply (respiration) with energy demand (protein synthesis) (see Materials and Methods, 'Allocation of energy to support the cost of protein synthesis with rising temperate'). The total area of each pie chart represents the energy from respiration (Fig. 4A–D: 329, 594, 286 and 476 µJ, respectively). The percentage allocation to protein synthesis is represented by the area in black within each pie chart. For example, Fig. 4A shows the energy allocation at a temperature of 18°C is 42% to protein synthesis for a 147 µm larva of family 9. This allocation is calculated as follows (from data in Figs 1E and 3D): (a) respiration rate of 679 pmol O_2 larva^{-1} day^{-1} (based on 28.3 pmol O_2 larva^{-1} h^{-1} at 18°C for family 9) converts to 329 µJ day^{-1} (679 pmol O_2×484 kJ mol^{-1} O_2÷1000); (b) protein synthesis rate of 65 ng protein larva^{-1} day^{-1} (based on 2.7 ng protein larva^{-1} h^{-1} at 18°C) converts to 137 µJ day^{-1} (65 ng protein×2.1 J mg^{-1} protein synthesized). Thus, the ratio of the energy required to support protein synthesis (137 µJ day^{-1}) to the total energy supply (329 µJ day^{-1}) is 42% (as presented in Fig. 4A). For the same-sized larvae from family 9 exposed to a higher temperature of 28°C (Fig. 4B), the high Q_{10} value of 2.4 for respiration would supply sufficient energy to meet the increased rate of protein synthesis at this higher temperature, as protein synthesis has a lower Q_{10} of 1.7 relative to respiration at 2.4.

The physiological state labeled 'optimal' (Fig. 4B) is the scenario where larvae from family 9 have sufficient energy to meet (and exceed) the increased metabolic cost from an increased rate of protein synthesis, which requires 28% of total energy at the higher temperature. Herein, 'optimal' is considered to be a scenario where 50% or less of ATP is allocated to a single process – protein synthesis in this case – allowing for sufficient energy in the ATP

pool to support other essential processes (e.g. ion regulation: Pan et al., 2018, 2021). In contrast, same-sized (147 µm) larvae from family 21 are considered to be in a 'stressful' physiological state at the same temperature (28°C; Fig. 4D). In this case, the cost of supporting the increased rate of protein synthesis requires an increased energy allocation from 34% at 18°C (Fig. 4C) to 67% at 28°C (Fig. 4D). It is notable in these scenarios that larvae from these two families allocate between 42% (family 9) and 34% (family 21) of total energy to protein synthesis. This sustainable physiological scenario at 18°C would permit allocation of cellular energy to other essential physiological processes in *C. gigas* larvae (e.g. the cost of ion transport and calcification; see Pan et al., 2018). It is only under conditions of rising temperature that the unsustainable physiological allocation to protein synthesis (67% at 28°C) becomes evident for family 21. Pan et al. (2021) provides a comparison of larval survival of *C. gigas* at 21°C and 28°C.

DISCUSSION

Following on from previous work (Pace et al., 2006; Hedgecock and Davis, 2007; Sun et al., 2015; Pan et al., 2021), this study aimed to develop phenotypic contrasts among different pedigreed larval families of the Pacific oyster (*Crassostrea gigas*). This offered a unique advantage for insights into biological variance and mechanisms of physiological resilience of marine organisms to environmental change. Of particular interest in the present study is the close relatedness of larval families 2 and 3 and their corresponding similarity in high Q_{10} values of respiration averaging ∼3.0 (Table 2, Fig. 2). These two larval families have a genetic relatedness of 0.375, because they share the same male parent (male C, Table 1), and sibling female parents (females D.1 and D.2, indicating different individuals of the same family line, Table 1) (see Materials and Methods). Thus, reproducibility of phenotypic measurements is found among replicate observations of the same family and among different larval families sharing parents. Overall, these data suggest that there is standing genetic variation for temperature sensitivity in current populations. The availability of these pedigreed lines will allow genetic mapping of physiological phenotypes in subsequent generations (e.g. the ability to map loci for viability in F_2 families of *C. gigas*: Yin and Hedgecock, 2021).

In our previous study (Pan et al., 2021), we reported a Q_{10} of ∼3 for the thermal sensitivity of protein synthesis rates in *C. gigas* larvae (from table 3 of that study, average Q_{10} of 2.9±0.18). This finding was based on an analysis of protein synthesis across 13 different larval sizes, representing seven different larval cohorts. In the present study, two mechanisms of resilience were identified. First, specific larval families were found to have increased thermal sensitivity of respiration (Fig. 2). Notably, these differences remained constant during growth (size independent) (Fig. 2). Second, an alternative strategy was identified, of decreased thermal sensitivity (Q_{10} value of 1.7) for protein synthesis (Fig. 3D). The observed crossover at a temperature of ∼20°C for larval families 9 and 21 (Fig. 3D) suggests a genotype-by-environment response for the change in protein synthesis rate with rising temperature. The outcome from these analyses is a unique approach to define a physiological basis for biological diversity within a species that permits optimal function for energy allocation with changing temperature (larval family 9, Fig. 4A,B). Larval family 9 exhibits an optimal phenotypic contrast to other larval families (e.g. larval family 21, Fig. 4C,D) regarding the physiological response to increased temperature.

While an increase in respiration rate with rising temperature will provide additional ATP to sustain essential physiological processes, the trade-off of having that capacity is the requirement for increased food intake to sustain elevated rates of respiration (see below). Considerations of genetic-based resilience, physiological trade-offs required to sustain the maintenance of metabolism and growth, and changes in food availability in the environment will help to improve models that predict survival under various scenarios of environmental change.

Energy allocation response to rising temperature

The current study identified two sets of related larval families of *C. gigas* (larval families 1 and 4, and 2 and 3) that have the physiological capacity to increase their respiration rate with a high thermal sensitivity (Fig. 2: Q_{10} value of ∼3) to match the demand for ATP from thermally induced increases in protein synthesis (which is known to have a Q_{10} of 3; Pan et al., 2021). Respiration Q_{10} values of 3 or higher are not uncommon for a range of freshwater, marine and terrestrial ectotherms (Seebacher et al., 2015). In the present study, of the 21 families tested, four had the physiological capacity to increase the Q_{10} of respiration to 3. Previously, Pan et al. (2021) reported that *C. gigas* larvae had high Q_{10} values for protein synthesis. Here, we report that specific larval families of *C. gigas* have the physiological capacity to match the increased ATP demand from protein synthesis with rising temperature with a corresponding increase in respiration. This physiology would confer resilience to rising temperature.

Findings for resilience in larval families of *C. gigas* have previously been shown for other environmental stressors, (e.g. ocean acidification: Frieder et al., 2017, 2018). In these cases (see also Pan et al., 2015, 2018), a common response mechanism is the regulation of protein turnover and the increased metabolic cost of increasing synthesis to balance protein metabolic dynamics (synthesis, turnover and accretion). Under optimal conditions, the fraction of energy allocated to protein synthesis reported in the present study (Fig. 4: 34–42%) is consistent with previous studies (Lee et al., 2016; Frieder et al., 2017; Pan et al., 2018, 2021). Fig. 4 also shows the energy not accounted for by protein synthesis in this analysis ('unaccounted'). For larval stages of *C. gigas*, this 'unaccounted' fraction has been well characterized biochemically, with the sodium pump (Na^+,K^+-ATPase activity), calcification and nucleic acid biosynthesis comprising the majority of the remaining energy not accounted for by protein synthesis (Pan et al., 2018). If one of these allocation values is altered in response to environmental change – such as protein synthesis increasing to 67% allocation under rising temperature (Fig. 4D: family 21) – support for other essential physiological processes will likely be compromised through energy limitation.

Energy trade-offs of high metabolic rates

The physiological strategy highlighted in the present study of increasing respiration rate to meet the demands of protein biosynthesis (Fig. 4) requires additional energy to fuel metabolism. Specifically, the increase in respiration at 28°C for larval family 9, which has a Q_{10} of 2.4, is 594 µJ day^{-1}. This increase in available energy is sufficient to meet the metabolic demand of protein synthesis at this higher temperature (Fig. 4B, 'optimal'). Conversely larval family 21, which has a respiration Q_{10} of 1.7, increased available energy to 476 µJ day^{-1}, an available energy that may be insufficient to support the physiological demand of other essential processes (Pan et al., 2018; 2021) beyond protein synthesis (Fig. 4D, 'stressful'). The difference in available energy between the optimal and stressful physiological state is 118 µJ. What amount of additional algal foods would be required to meet that energy difference?

Three of the common algal foods used to grow larvae of *C. gigas* have a similar organic weight (from table 1 of Helm and Bourne, 2004: *Isochrysis galbana*, *T-ISO*, *Pavlova lutheri*). Droop et al. (1982) report a value of 0.54 µJ cell^{-1} of *P. lutheri*. Using this estimate, the number of algal cells required to fuel a differential energy of 118 µJ is 219 algal cells per day (9 per hour, assuming 100% efficiency of energy conversion). Larvae of *C. gigas* grown on a similar algal ration to that used in the present study (30,000 cells ml^{-1}) had a feeding rate of 30 cells h^{-1} (Pace et al., 2006: ∼150 µm larva). This would need to be increased to 39 cells h^{-1} to provide the additional energy required to sustain the optimal energy amount of larval family 9 (assuming similar feeding and assimilation rates). This increase in feeding rate is physiologically feasible (see Pace et al., 2006, for studies of genetically determined variation in feeding and assimilation rates in *C. gigas* larvae). Information remains scant regarding the actual amounts of food available to support larval growth in the ocean (Crisp et al., 1985; Fenaux et al., 1994; see p. 639 of Bayne, 2017, for a review of more recent literature). In addition, major changes are anticipated in global phytoplankton species, production and biochemical composition in a warming ocean (Behrenfeld et al., 2016; Holm et al., 2022). The energy allocation model presented in Fig. 4 illustrates the physiological capacity to respond to ocean change. Integrating such physiological capacities into long-term monitoring and models of environmental change will assist in predicting 'winners' and 'losers' within populations of a single species.

Differential thermal sensitivity of protein synthesis

Denaturation of proteins is time dependent: the longer an enzyme subsists in higher temperatures, the more likely it is that denaturation will occur (Schulte, 2015). Additionally, small changes in temperature have large impacts on protein conformation (Dong et al., 2022). At higher temperature, proteins are more likely to be changing between conformations, and are less likely to be in a proper conformation to perform designated functions. Thus, protein synthesis rates would need to be increased to maintain the same number of proteins capable of performing their function at a given moment in time. In *C. gigas*, all 88 *Hsp70* heat shock genes in the genome show increased expression in response to thermal stress (Zhang et al., 2012). In the fruit fly *Drosophila melanogaster*, a higher number of the heat shock protein gene copies incur additional metabolic cost (Hoekstra and Montooth, 2013).

RNA structures can impact the regulation of protein synthesis rate (Mortimer et al., 2014). In response to heat shock, RNA secondary structure is involved in regulating gene expression (Su et al., 2018). Across a range of species of marine mollusks, Liao et al. (2021) have shown that stability of mRNA secondary structure (based on nucleotide sequence) differs adaptively among species across a wide temperature range. In our study of larval families of *C. gigas*, we identified a family that had a lower Q_{10} value for protein synthesis (larval family 9, Fig. 4). We suggest that such larval families may have mRNA structures that result in a lower response of protein synthesis to higher temperature. Further studies are required to test the possibility that these structural changes would result in a rapid increase in translation with rising temperature, and that there is genetic variation associated with this process. In the current study, it has been established that high Q_{10} values for protein synthesis require a substantial amount of energy to support increased rates with rising temperature (Fig. 4D). Conversely, a lower temperature sensitivity for protein synthesis would result in lower energy costs, and a more optimal allocation of ATP (Fig. 4B). This latter ('optimal') physiology would reduce the requirement to increase synthesis rates with rising temperature.

An analysis of fractional rates of protein synthesis supports this suggestion. Specifically, larval families 9 and 21 are of similar size and protein content (147 µm and 66 ng protein per larva). The rate of protein synthesis at 28°C was 3.3 and 6.3 ng protein larva^{-1} h^{-1} for larval families 9 and 21, respectively. This equates to a 2-fold difference in fractional rates of protein synthesis [family 9: 5% (3.3÷66); family 21: 10% (6.3÷66)]. These two larval families had similar growth rates (same size and protein content for a given age), hence the 2-fold higher fractional rate of protein synthesis for larval family 21 would represent a higher turnover rate of protein (i.e. protein degradation rate). The cost of this apparent protein instability is reflected in the increased allocation required to support protein synthesis (Fig. 4: family 9, 28%; family 21, 67%). As discussed above, these differences in temperature-dependent physiological and biochemical rates among larval families of *C. gigas* may reflect standing genetic variation, where the phenotype is a change in biochemical strategies of protein synthetic dynamics (synthesis, degradation, accretion). Increased protein turnover, not resulting in increased protein accretion, appears to be a common mechanism for the stress response in developmental stages of marine invertebrates. For instance, in larval stages of *C. gigas* and the sea urchin *Stronglyocentrotus purpuratus*, increased rates of protein turnover occurred under ocean acidification treatments (Pan et al., 2015; Frieder et al., 2018). Given the large number of 88 *Hsp70* heat shock genes in the genome of *C. gigas*, it would certainly be of interest in future studies to link the physiology of the thermal sensitivity of protein synthesis to the biochemistry of changes in specific proteins of larval stages.

Identification of 'winners' under environmental change scenarios

The ability of a species to cope with environmental change sets the evolutionary potential of 'winners and losers' (Somero, 2010). The genetic and physiological basis of adaptation to environmental change is highly complex, making predictions across generations particularly challenging. As highlighted by Somero (2010), few studies directly address this question by rearing animals across generations and measuring their physiology. The phenotypic similarity of larval families 1–4 in terms of high respiration Q_{10} values (Table 2) and the close relatedness among these families (Table 1) suggest an additive genetic component to Q_{10} variance. This further implies that animals with the trait of high respiration Q_{10} values would likely contribute to the greater physiological resilience of an evolving natural population. In contrast to this classic scenario of directional selection on additive genetic variation, however, our finding of lower Q_{10} values in G_1 compared with G_0 larval families suggests that there is also a substantial non-additive genetic component to variation in respiration Q_{10}. Non-additive genetic variation for a complex physiological trait – growth in larvae of *C. gigas* – was previously evidenced by hybrid vigor in crosses among inbred parent lines (Pace et al., 2006). Transgenerational evidence for non-additive and, therefore, non-heritable variation in respiration Q_{10} is seen by comparing the findings of Pan et al. (2021) with those of the present study. Pan et al. (2021) report that a cohort of larvae (cohort 5, a full-sibling G_0 family) had a Q_{10} value of 3.0. That cohort of larvae was reared to adulthood and the sibling broodstock spawned for the present study, yielding family 13. Notably, the high Q_{10} value of 3.0 for respiration in the previous generation (Pan et al., 2021: cohort 5) was not evident in the next generation used in the present study

(Table 2: family 13, Q_{10}=2.2 and 2.1 for larvae of different sizes; Fig. 2). These examples of non-additive genetic effects have important implications for transgenerational inheritance of complex traits and warrant caution regarding predicting inheritance of physiological resilience solely based on parental phenotypes (presumed 'winners'). A focus on transgenerational (egg-to-egg) inheritance of physiological traits that provide thermal tolerance would significantly advance our understanding of and ability to predict resilience under various scenarios of future climate change.

For studies of biological responses to global ocean change, the study of bivalves (such as *C. gigas* as a model organism) provides the availability for reproducible analyses of existing genetic lines (cf. wild-type), and has well-developed genomic and physiological resources. Additionally, *C. gigas* has a global ecological distribution across six continents and tolerates a wide temperature range (2–35°C: Helm, 2009; Miossec et al., 2009). Of note is that the aquaculture of bivalves offers great potential as a source of future 'blue food' (Nature editorial, 2021; Naylor et al., 2021), given their high nutritional quality as a human dietary source. The future success of producing blue food will depend upon understanding the basic biology and resilience potential of farmed species. Although the present study was not specifically designed to allow quantitative dissection and analysis of genetic-based variation, the finding that several extant larval families have biochemical strategies of differential energy allocation to respond to rising temperature is notable, regarding the identification of resilient phenotypes. For future analyses, the experimental approaches presented here offer the potential to address questions of physiological resilience and genetic-based adaptation to global ocean change.

Acknowledgements
We are especially grateful to our colleague Dr Dennis Hedgecock for his intellectual input on this project and for insightful comments on earlier drafts of the manuscript. Special thanks to our industry partner, Thomas Grimm, and his dedicated staff at Carlsbad Aquafarm, without whose facilities, support and collaboration the long-term maintenance of pedigreed lines used in this study would not have been possible. Our thanks to the staff of the Wrigley Marine Science Center at the University of Southern California for their assistance in supporting the larval culturing work reported here. D.T.M. would like to dedicate this publication to his recently deceased mother, Mrs. Pamela Manahan.

Competing interests
The authors declare no competing or financial interests.

Author contributions
Conceptualization: M.B.D., F.T.C.P., A.W.G., N.L., D.T.M.; Methodology: M.B.D., F.T.C.P., A.W.G., N.L., D.T.M.; Validation: D.T.M.; Formal analysis: M.B.D., F.T.C.P., A.W.G., N.L., D.T.M.; Investigation: M.B.D., F.T.C.P., A.W.G., N.L., D.T.M.; Resources: D.T.M.; Data curation: M.B.D., F.T.C.P., A.W.G., N.L., D.T.M.; Writing - original draft: M.B.D., D.T.M.; Writing - review & editing: M.B.D., F.T.C.P., A.W.G., N.L., D.T.M.; Visualization: D.T.M.; Supervision: D.T.M.; Project administration: D.T.M.; Funding acquisition: D.T.M.

Funding
This work was supported, in part, by National Science Foundation grants to D.T.M.

References
Applebaum, S. L., Pan, T. C. F., Hedgecock, D. and Manahan, D. T. (2014). Separating the nature and nurture of the allocation of energy in response to global change. *Integr. Comp. Biol.* **54**, 284-295. doi:10.1093/icb/icu062

Bayne, B. L. (2017). *Biology of Oysters*. Academic Press.

Behrenfeld, M. J., O'malley, R. T., Boss, E. S., Westberry, T. K., Graff, J. R., Halsey, K. H., Milligan, A. J., Siegel, D. A. and Brown, M. B. (2016). Revaluating ocean warming impacts on global phytoplankton. *Nat. Clim. Change* **6**, 323-330. doi:10.1038/nclimate2838

Berrigan, D. and Partridge, L. (1997). Influence of temperature and activity on the metabolic rate of adult *Drosophila melanogaster*. *Comp. Biochem. Physiol. A Physiol.* **118**, 1301-1307. doi:10.1016/S0300-9629(97)00030-3

Bradford, M. M. (1976). A rapid and sensitive method for the quantitation of microgram quantities of protein utilizing the principle of protein-dye binding. *Anal. Biochem.* **72**, 248-254. doi:10.1016/0003-2697(76)90527-3

Breese, W. P. and Malouf, R. E. (1975). *Hatchery Manual for the Pacific Oyster*. Corvallis, OR, USA: Oregon State University Sea Grant College Program.

Cherkasov, A. S., Biswas, P. K., Ridings, D. M., Ringwood, A. H. and Sokolova, I. M. (2006). Effects of acclimation temperature and cadmium exposure on cellular energy budgets in the marine mollusk *Crassostrea virginica*: linking cellular and mitochondrial responses. *J. Exp. Biol.* **209**, 1274-1284. doi:10.1242/jeb.02093

Crisp, D. J., Yule, A. B. and White, K. N. (1985). Feeding by oyster larvae: the functional response, energy budget and a comparison with mussel larvae. *J. Mar. Biol. Assoc. UK* **65**, 759-783. doi:10.1017/S0025315400052589

Dahlke, F. T., Wohlrab, S., Butzin, M. and Pörtner, H. O. (2020). Thermal bottlenecks in the life cycle define climate vulnerability of fish. *Science* **369**, 65-70. doi:10.1126/science.aaz3658

Dong, Y. W., Liao, M. L., Han, G. D. and Somero, G. N. (2022). An integrated, multi–level analysis of thermal effects on intertidal molluscs for understanding species distribution patterns. *Biol. Rev.* **97**, 554-581. doi:10.1111/brv.12811

Dupont, S., Dorey, N. and Thorndyke, M. (2010). What meta-analysis can tell us about vulnerability of marine biodiversity to ocean acidification? *Estuar. Coast. Shelf Sci.* **89**, 182-185. doi:10.1016/j.ecss.2010.06.013

Droop, M. R., Mickelson, M. J., Scott, J. M. and Turner, M. F. (1982). Light and nutrient status of algal cells. *J. Mar. Biolog. Assoc. UK* **62**, 403-434. doi:10.1017/S0025315400057362

Einum, S., Fossen, E. I., Parry, V. and Pélabon, C. (2019). Genetic variation in metabolic rate and correlations with other energy budget components and life history in *Daphnia magna*. *Evol. Biol.* **46**, 170-178. doi:10.1007/s11692-019-09473-x

Fenaux, L., Strathmann, M. F. and Strathmann, R. A. (1994). Five tests of food–limited growth of larvae in coastal waters by comparisons of rates of development and form of echinoplutei. *Limnol. Oceanogr.* **39**, 84-98. doi:10.4319/lo.1994.39.1.0084

Folk, D. G., Hoekstra, L. A. and Gilchrist, G. W. (2007). Critical thermal maxima in knockdown-selected *Drosophila*: are thermal endpoints correlated? *J. Exp. Biol.* **210**, 2649-2656. doi:10.1242/jeb.003350

Fossen, E. I., Pélabon, C. and Einum, S. (2019). Genetic and environmental effects on the scaling of metabolic rate with body size. *J. Exp. Biol.* **222**, jeb193243. doi:10.1242/jeb.193243

Frieder, C. A., Applebaum, S. L., Pan, T.-C. F., Hedgecock, D. and Manahan, D. T. (2017). Metabolic cost of calcification in bivalve larvae under experimental ocean acidification. *ICES J. Mar. Sci.* **74**, 941-954. doi:10.1093/icesjms/fsw213

Frieder, C. A., Applebaum, S. L., Pan, T.-C. F. and Manahan, D. T. (2018). Shifting balance of protein synthesis and degradation sets a threshold for larval growth under environmental stress. *Biol. Bull.* **234**, 45-57. doi:10.1086/696830

Gnaiger, E. (1983). Calculation of energetic and biochemical equivalents of respiratory oxygen consumption. In *Polarographic Oxygen Sensors: Aquatic and Physiological Applications* (ed. E Gnaiger and H Forstner), pp. 337-345. Berlin: Springer.

Hand, S. C. (1999). Calorimetric approaches to animal physiology and bioenergetics. In *Handbook of Thermal Analysis and Calorimetry* (ed. R. B. Kemp), pp. 469-510. Amsterdam: Elsevier Science.

Hand, S. C. and Hardewig, I. (1996). Downregulation of cellular metabolism during environmental stress: mechanisms and implications. *Annu. Rev. Physiol.* **58**, 539-563. doi:10.1146/annurev.ph.58.030196.002543

Hawkins, A. J. S. (1991). Protein turnover: a functional appraisal. *Funct. Ecol.* **5**, 222-233. doi:10.2307/2389260

Haws, M. C., Dimichele, L. and Hand, S. C. (1993). Biochemical changes and mortality during metamorphosis of the Eastern oyster, *Crassostrea virginica*, and the Pacific oyster, *Crassostrea gigas*. *Mol. Mar. Biol. Biotech.* **2**, 207-217.

Hedgecock, D. and Davis, J. P. (2007). Heterosis for yield and crossbreeding of the Pacific oyster *Crassostrea gigas*. *Aquaculture* **272**, S17-S29. doi:10.1016/j.aquaculture.2007.07.226

Hedgecock, D., Mcgoldrick, D. J. and Bayne, B. L. (1995). Hybrid vigor in Pacific oysters: an experimental approach using crosses among inbred lines. *Aquaculture* **137**, 285-298. doi:10.1016/0044-8486(95)01105-6

Helm, M. M. (2009). *Crassostrea gigas*. In Cultured aquatic species fact sheets. FAO, Rome, Italy. https://www.fao.org/fishery/docs/DOCUMENT/aquaculture/CulturedSpecies/file/en/en_pacificcuppedoyster.htm.

Helm, M. M. and Bourne, N. (2004). Hatchery culture of bivalves: A practical manual. FAO Fisheries Technical Paper No. 471. FAO, Rome, Italy.

Hoekstra, L. A. and Montooth, K. L. (2013). Inducing extra copies of the Hsp70 gene in *Drosophila melanogaster* increases energetic demand. *BMC Evol. Biol.* **13**, 68. doi:10.1186/1471-2148-13-68

Holm, H. C., Fredricks, H. F., Bent, S. M., Lowenstein, D. P., Ossolinski, J. E., Becker, K. W., Johnson, W. M., Schrage, K. and Van Mooy, B. A. S. (2022). Global ocean lipidomes show a universal relationship between temperature and lipid unsaturation. *Science* **376**, 1487-1491. doi:10.1126/science.abn7455

Jaeckle, W. B. and Manahan, D. T. (1989). Growth and energy imbalance during the development of a lecithotrophic molluscan larva (*Haliotis rufescens*). *Biol. Bull.* **177**, 237-246. doi:10.2307/1541939

Kalinowski, S. T., Taper, M. L. and Marshall, T. C. (2007). Revising how the computer program CERVUS accommodates genotyping error increases success in paternity assignment. *Mol. Ecol.* **16**, 1099-1106. doi:10.1111/j.1365-294X.2007.03089.x

Lee, J. W., Applebaum, S. L. and Manahan, D. T. (2016). Metabolic cost of protein synthesis in larvae of the Pacific oyster (*Crassostrea gigas*) is fixed across genotype, phenotype, and environmental temperature. *Biol. Bull.* **230**, 175-187. doi:10.1086/BBLv230n3p175

Liao, M.-L., Dong, Y.-W. and Somero, G. N. (2021). Thermal adaptation of mRNA secondary structure: stability versus lability. *Proc. Natl. Acad. Sci. USA* **118**, e2113324118. doi:10.1073/pnas.2113324118

Lynch, M. and Walsh, B. (1998). *Genetics and Analysis of Quantitative Traits*. Sunderland, MA: Sinnauer Associates.

Melzner, F., Gutowska, M. A., Langenbuch, M., Dupont, S., Lucassen, M., Thorndyke, M. C., Bleich, M. and Pörtner, H. O. (2009). Physiological basis for high CO2 tolerance in marine ectothermic animals: pre-adaptation through lifestyle and ontogeny? *Biogeosciences* **6**, 2313-2331. doi:10.5194/bg-6-2313-2009

Miossec, L., Le Deuff, R. M. and Goulletquer, P. (2009). Alien species alert: *Crassostrea gigas* (Pacific oyster). *ICES Cooperative Res. Rep.* **299**, 42. doi:10.17895/ices.pub.5417

Moran, A. L. and Manahan, D. T. (2004). Physiological recovery from prolonged 'starvation' in larvae of the Pacific oyster *Crassostrea gigas*. *J. Exp. Mar. Bio. Ecol.* **306**, 17-36. doi:10.1016/j.jembe.2003.12.021

Mortimer, S. A., Kidwell, M. A. and Doudna, J. A. (2014). Insights into RNA structure and function from genome-wide studies. *Nat. Rev. Genet.* **15**, 469-479. doi:10.1038/nrg3681

Nature Editorial. (2021). Harness the world's 'blue' food systems to help end hunger. *Nature* **597**, 303. doi:10.1038/d41586-021-02476-9

Naylor, R. L., Hardy, R. W., Buschmann, A. H., Bush, S. R., Cao, L., Klinger, D. H., Little, D. C., Lubchenco, J., Shumway, S. E. and Troell, M. (2021). A 20-year retrospective review of global aquaculture. *Nature* **591**, 551-563. doi:10.1038/s41586-021-03308-6

Pace, D. A. and Manahan, D. T. (2006). Fixed metabolic costs for highly variable rates of protein synthesis in sea urchin embryos and larvae. *J. Exp. Biol.* **209**, 158-170. doi:10.1242/jeb.01962

Pace, D. A., Marsh, A. G., Leong, P. K., Green, A. J., Hedgecock, D. and Manahan, D. T. (2006). Physiological bases of genetically determined variation in growth of marine invertebrate larvae: a study of growth heterosis in the bivalve *Crassostrea gigas*. *J. Exp. Mar. Biol. Ecol.* **335**, 188-209. doi:10.1016/j.jembe.2006.03.005

Pan, T.-C. F., Applebaum, S. L. and Manahan, D. T. (2015). Experimental ocean acidification alters the allocation of metabolic energy. *Proc. Natl. Acad. Sci. USA* **112**, 4696-4701. doi:10.1073/pnas.1416967112

Pan, T.-C. F., Applebaum, S. L., Frieder, C. A. and Manahan, D. T. (2018). Biochemical bases of growth variation during development: a study of protein turnover in pedigreed families of bivalve larvae (*Crassostrea gigas*). *J. Exp. Biol.* **221**, jeb171967. doi:10.1242/jeb.171967

Pan, T.-C. F., Applebaum, S. L. and Manahan, D. T. (2021). Differing thermal sensitivities of physiological processes alter ATP allocation. *J. Exp. Biol.* **224**, jeb233379. doi:10.1242/jeb.233379

Penn, J. L. and Deutsch, C. (2022). Avoiding ocean mass extinction from climate warming. *Science* **376**, 524-526. doi:10.1126/science.abe9039

Pörtner, H. O. (2002). Climate variations and the physiological basis of temperature dependent biogeography: systemic to molecular hierarchy of thermal tolerance in animals. *Comp. Biochem. Physiol. A Mol. Integr. Physiol.* **132**, 739-761. doi:10.1016/S1095-6433(02)00045-4

Pörtner, H. O. and Knust, R. (2007). Climate change affects marine fishes through the oxygen limitation of thermal tolerance. *Science* **315**, 95-97. doi:10.1126/science.1135471

Quayle, D. B. (1988). Pacific oyster culture in British Columbia. *Can. Bull. Fish. Aquat. Sci.* **218**, 1-241.

Ross, P. M., Parker, L., O'connor, W. A. and Bailey, E. A. (2011). The impact of ocean acidification on reproduction, early development and settlement of marine organisms. *Water* **3**, 1005-1030. doi:10.3390/w3041005

Schmidt-Nielsen, K. (1997). *Animal Physiology: Adaptation and Environment*, 5th edn. Cambridge University Press.

Schulte, P. M. (2015). The effects of temperature on aerobic metabolism: towards a mechanistic understanding of the responses of ectotherms to a changing environment. *J. Exp. Biol.* **218**, 1856-1866. doi:10.1242/jeb.118851

Seebacher, F., White, C. R. and Franklin, C. E. (2015). Physiological plasticity increases resilience of ectothermic animals to climate change. *Nat. Clim. Change* **5**, 61-66. doi:10.1038/nclimate2457

Siems, W. G., Schmidt, H., Gruner, S. and Jakstadt, M. (1992). Balancing of energy–consuming processes of K 562 cells. *Cell Biochem. Funct.* **10**, 61-66. doi:10.1002/cbf.290100110

Sokolova, I. (2021). Bioenergetics in environmental adaptation and stress tolerance of aquatic ectotherms: linking physiology and ecology in a multi-stressor landscape. *J. Exp. Biol.* **224**, jeb236802. doi:10.1242/jeb.236802

Sokolova, I. M., Frederich, M., Bagwe, R., Lannig, G. and Sukhotin, A. A. (2012). Energy homeostasis as an integrative tool for assessing limits of environmental stress tolerance in aquatic invertebrates. *Mar. Environ. Res.* **79**, 1-15. doi:10.1016/j.marenvres.2012.04.003

Somero, G. N. (2010). The physiology of climate change: how potentials for acclimatization and genetic adaptation will determine 'winners' and 'losers'. *J. Exp. Biol.* **213**, 912-920. doi:10.1242/jeb.037473

Somero, G. N., Lockwood, B. L. and Tomanek, L. (2017). *Biochemical Adaptation: Response to Environmental Challenges, From Life's Origins to the Anthropocene*. Sinauer Associates.

Su, Z., Tang, Y., Ritchey, L. E., Tack, D. C., Zhu, M., Bevilacqua, P. C. and Assmann, S. M. (2018). Genome-wide RNA structurome reprogramming by acute heat shock globally regulates mRNA abundance. *Proc. Natl. Acad. Sci. USA* **115**, 12170-12175. doi:10.1073/pnas.1807988115

Sun, X., Shin, G. and Hedgecock, D. (2015). Inheritance of high-resolution melting profiles in assays targeting single nucleotide polymorphisms in protein-coding sequences of the Pacific oyster *Crassostrea gigas*: implications for parentage assignment of experimental and commercial broodstocks. *Aquaculture* **437**, 127-139. doi:10.1016/j.aquaculture.2014.11.009

Taylor, J. G. (1982). *An Introduction to Error Analysis*. Mill Valley: University Science.

Tresguerres, M. (2016). Novel and potential physiological roles of vacuolar-type H^+-ATPase in marine organisms. *J. Exp. Biol.* **219**, 2088-2097. doi:10.1242/jeb.128389

Tsukada, M. and Ohsumi, Y. (1993). Isolation and characterization of autophagy-defective mutants of *Saccharomyces cerevisiae*. *FEBS Lett.* **333**, 169-174. doi:10.1016/0014-5793(93)80398-E

Vavra, J. and Manahan, D. T. (1999). Protein metabolism in lecithotrophic larvae (Gastropoda: *Haliotis rufescens*). *Biol. Bull.* **196**, 177-186. doi:10.2307/1542563

Wieser, W. and Krumschnabel, G. (2001). Hierarchies of ATP-consuming processes: direct compared with indirect measurements, and comparative aspects. *Biochem* **355**, 389-395. doi:10.1042/bj3550389

Williams, C. M., Szejner-Sigal, A., Morgan, T. J., Edison, A. S., Allison, D. B. and Hahn, D. A. (2016). Adaptation to low temperature exposure increases metabolic rates independently of growth rates. *Integr. Comp. Biol.* **56**, 62-72. doi:10.1093/icb/icw009

Yin, X. and Hedgecock, D. (2021). Overt and concealed genetic loads revealed by QTL mapping of genotype-dependent viability in the Pacific oyster *Crassostrea gigas*. *Genetics* **219**, iyab165. doi:10.1093/genetics/iyab165

Zhang, G., Fang, X., Guo, X., Li, L. I., Luo, R., Xu, F., Yang, P., Zhang, L., Wang, X., Qi, H. et al. (2012). The oyster genome reveals stress adaptation and complexity of shell formation. *Nature* **490**, 49-54. doi:10.1038/nature11413